Article

Coastal Flood Assessment due to sea level rise and extreme storm events - Case study of the Atlantic Coast of Portugal Mainland

Carlos Antunes [1,2,*], Carolina Rocha [2] and Cristina Catita [1,2]

[1] Instituto Dom Luiz, Universidade de Lisboa
[2] Faculdade de Ciências, Universidade de Lisboa
* Correspondence: cmantunes@fc.ul.pt;

Received: date; Accepted: date; Published: date

Abstract: Portugal Mainland has hundreds of thousands of people living in the Atlantic coastal zone, with numerous high economic value activities and a high number of infrastructures that must be protected from natural coastal hazard, namely extreme storms and sea level rise (SLR). In the context of climate change adaptation strategies, a reliable and accurate assessment of the physical vulnerability to SLR is crucial. This study is a contribution to the implementation of flooding standards imposed by the European Directive 2007/60/EC, which requires each member state to assess the risk associated to SLR and floods caused by extreme events. Therefore, coastal hazard in the Continental Atlantic coast of Portugal Mainland was evaluated for 2025, 2050 and 2100 in the whole coastal extension with different sea level scenarios for different extreme event return periods and due to SLR. A coastal flooding probabilistic map was produced based on the developed methodology using Geographic Information Systems (GIS) technology. The Extreme Flood Hazard Index (EFHI) was determined on flood probabilistic bases through five probability intervals of 20% of amplitude. For a given SLR scenario, the EFHI is expressed, on the probabilistic flooding maps for an extreme tidal maximum level, by five hazard classes ranging from 1 (Very Low) to 5 (Extreme).

Keywords: Sea Level Rise; Coastal Flood Hazard; Storm Surge; Extreme Tidal Level; GIS.

1. Introduction

Sea level rise (SLR), as consequence of global warming, has been occurring for more than a century. For a global temperature anomaly increase of around 1 °C, the Global Mean Sea Level (GMSL) has raised around 20 cm since the end of the 19th century, both globally and regionally [1-4]. Sea Level Rise (SLR) in west coast of Portugal Mainland is in line with GMSL, with a slow and progressive response to global warming [5]. On one hand, this is due to the oceans thermal expansion and, on the other hand, and in a smaller extent, to the ocean mass increase resulting from the melting of the continental glaciers and of the Greenland and Antarctica polar ice caps. However, the most recent data from the GRACE satellites mission and the ARGO float network indicate that since the beginning of this century the ocean mass component increase has already surpassed thermal expansion increase [4,6-8].

Due to the well-known ocean's inertia, with a slow response to global warming, SLR will continue to rise beyond the end of the 21st century. Even if global warming stops in the short term, the ocean would continue to rise due to the slow response of deep ocean warming and the melting dynamics of the glacier systems, either continental or Greenland and Antarctica.

The high exposure of the world's population that live along the coastal areas with less than 10 meters above mean sea level (MSL), that represents around 10% of world population and 13% of urban population [9] with a higher share on the least developed countries (14%), as well as the high importance of a large number of infrastructures, namely, harbors and maritime transportation

infrastructures, economic activities, business, industry, tourism and services (mainly in estuaries, deltas and inlet areas), in the context of climate change, makes the subject of SLR assessment a current and of highly important issue with strong socio-economic impacts in a near future.

Through the Floods Directive 2007/60/EC [10], the European Parliament and Council of the European Union requires each Member State to carry out a preliminary assessment to identify the river basins and associated coastal areas with a significant flooding risk due to climate changes. For such zones, the Member States need to draw up flood risk maps and establish flood risk management plans focused on prevention, protection and preparedness. The European Commission (EC) Directive applies to inland waters and all coastal waters across the whole territory of the European Union (EU).

Within the framework of this Directive requirements, the authors have been developing a methodology to produce coastal flood maps expressing coastal flooding hazard resulting from the combination of SLR and extreme values of coastal forcing. This ACPM extreme flooding hazard assessment is crucial to produce the corresponding coastal vulnerability and risk cartography. Modeling several physical parameters, such as the tides measured in the Portuguese coastal harbors, the meteorological forcing factors and the future SLR evaluation for 2050 and 2100, as well as the respective uncertainties, allows the model coupling through a probabilistic approach and consequently to the probabilistic flood hazard maps.

The ACPM coastal flood hazard assessment enables a wider physical vulnerability assessment at national scale [11], and regional case studies for inlet areas of the estuaries systems, such as the Ria de Aveiro (Northwest), Tagus Estuary (Lisbon region) [12] and the Ria Formosa (South). These studies at academic level, together with similar more detailed studies based on higher spatial resolution data (Municipal service contracts), have contributed to the development of methodologies and algorithms to obtain final products such as coastal flooding probabilistic maps, approached in this study, and coastal vulnerability and risk maps that will be published in near future.

The present work describes the developed methodology to produce coastal flooding cartography for Portugal mainland considering extreme forcing and maximum high-water level. Flooding cartography is based on the most updated topographic model, without inferring any coastal profile morphodynamics and nor considering coastline retrieving due to present and future erosion. The difficulty and complexity of such coastal morphologic modeling, due to a variety of factors and constrains (natural and human cause), would disable a country-wide high-resolution coastal risk assessment in such a limited time.

The developed methodology uses a hydrostatic flood model (usually called “bathtub model”) rather than a hydrodynamic flood model (computer-based dynamic water flow model), due to its simplicity when applying GIS and also because it does not requires the use of an accurate high-resolution digital topo-bathymetric model, which is often not available at national scale. [13] has demonstrated that the differences between hydrostatic and hydrodynamic models are moderate at regional scale and large in a few locations for tropical cyclones, due to friction, wind and other dynamic factors that affects the horizontal flood movement, however, yet small for extratropical cyclones which is the case of most storms that reach the ACPM.

2. Materials and Methods

2.1. Coastal flood forcing

2.1.1. Sea level rise projections

Data from the Cascais tide gauge (TG), the oldest gauge in Portugal and in all Iberian Peninsula, working since 1882, was used to estimate the first relative SLR empirical projection for the Portuguese coast by [14]. The gauge is located at open coast (Figure 2), at a site of low tectonic activity [15], reduced glacial isostatic adjustment (GIA) and with sea level in a considerable agreement with GSLR records [5].

Preprints (www.preprints.org) | NOT PEER-REVIEWED | Posted: 6 May 2019 doi:10.20944/preprints201905.0052.v1

Peer-reviewed version available at Geosciences 2019, 9, 239; doi:10.3390/geosciences9050239

Furthermore, [16], based on a daily average data series, concluded that the relative SLR at Cascais exhibited a rate of 4.1 mm/year for the past 12 years, demonstrated the correlation between Cascais TG with GMSL rates. The Cascais SLR analysis validation was performed by comparison results with regional and global data models obtained from satellite and global tide gauge data, after removing the difference of the corresponding vertical velocity rate effect (obtained from tectonics and GIA) [5].

For different MSL data series and different methodological approaches, [5] show a set of relative SLR projections for the 21st century, based on which the author generated a probabilistic ensemble used to compute a SLR probability density function at epoch 2100.

Based on the Cascais TG relative SLR estimation of 2.1 mm/year between 1992 and 2005 and 4.1 mm/year between 2006 and 2016, [5] estimated an accelerated SLR model, designated by Mod.FC_2b. The central estimate of this model (Figure 1) show an intermediate hazard projection, when compared with other estimations and extreme values reported by [4], with a value of 1.14 ± 0.15 m for epoch 2100. This Cascais TG projection model of SLR was applied to the entire ACPM to produce coastal flood probabilistic maps, used consequently for coastal vulnerability and risk assessment [10,11].

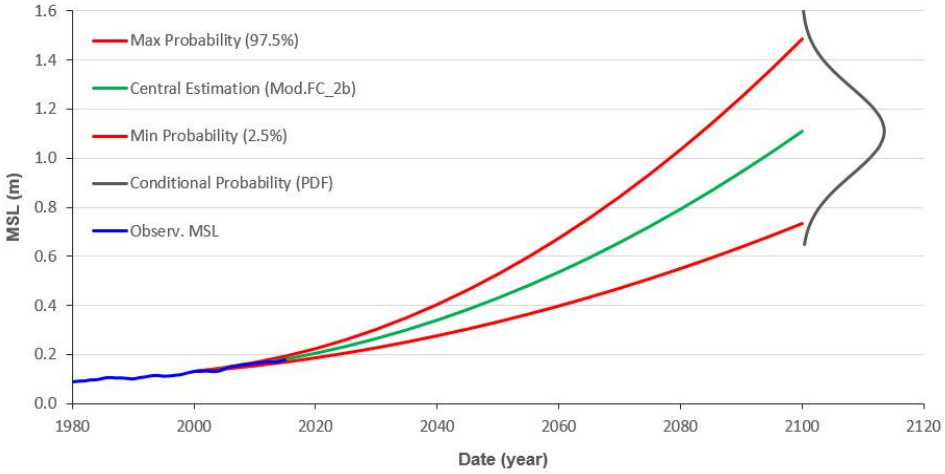

Figure 1. Model of relative SLR projection, Mod.FC_2b (Model 2b of FCUL), based on the analysis of Cascais tide gauge data series, from 1992 to 2016 [5].

2.1.2. Maximum tide modelling

Longest tide series in Portugal are only available for the Cascais and Lagos TG, under the responsibility of the national Directorate-General for the Territorial Development (DGT). For the rest of the country, except for the Leixões harbor (North), the tides were only observed for short periods of a few years to two decades in the tide gauges under the responsibility of the Portuguese Hydrographic Institute (IH).

All tidal data, by convention, are referred to the vertical reference used in hydrography, the chart datum (CD), defined in Portugal as the lowest low-tide (minimum low water) observed during a period longer than 19 years (18.6-year Moon's nodal period), plus an additional safety margin (a foot). For all Portuguese tide ports, the CD is 2.00 m relative to the national vertical reference, the 1938 Cascais Vertical Datum (CASCAIS1938), except for the Tagus Estuary, where the CD is 2.08 m. CD must be removed from the hydrographic tide heights to obtain the tide elevation, which corresponds to the tide orthometric height relative to the national vertical reference of CASCAIS1938.

Knowing that the maximum High Tide has a synoptic variation of 4 to 5 years (1/4 of Moon's nodal period), the annual reference tide for this study corresponds to a maximum high-water level, corresponding to the maximum of the equinoctial high tides. These maximum high tides occur when the Moon's perigee is closer to the Earth (denominated "Giant Moon" or "Super Moon" years),

causing the known "giant tides" or "king tides". For this reason, the 2010 king tides chosen for this national study.

To enable a rapid and comprehensive assessment study, four tidal harbors, namely *Leixões*, *Cascais*, *Sines* and *Lagos*, were chosen to estimate tides for the North, Center, Alentejo and Algarve regions of the ACPM (Figure 2). This partition into four tidal zones, as it will be explained further, contributed also for the terrain data model simplification, enabling the entire coastal extension assessment using 20 m spatial resolution data without exceeding computing capacity demand.

Tide models from [17] were used to model four regional tides for the 2010reference year, from which cumulative density functions (accumulated frequency or percentile function) were determined (lower curve in the Figure 5, for the case of the Cascais TG).

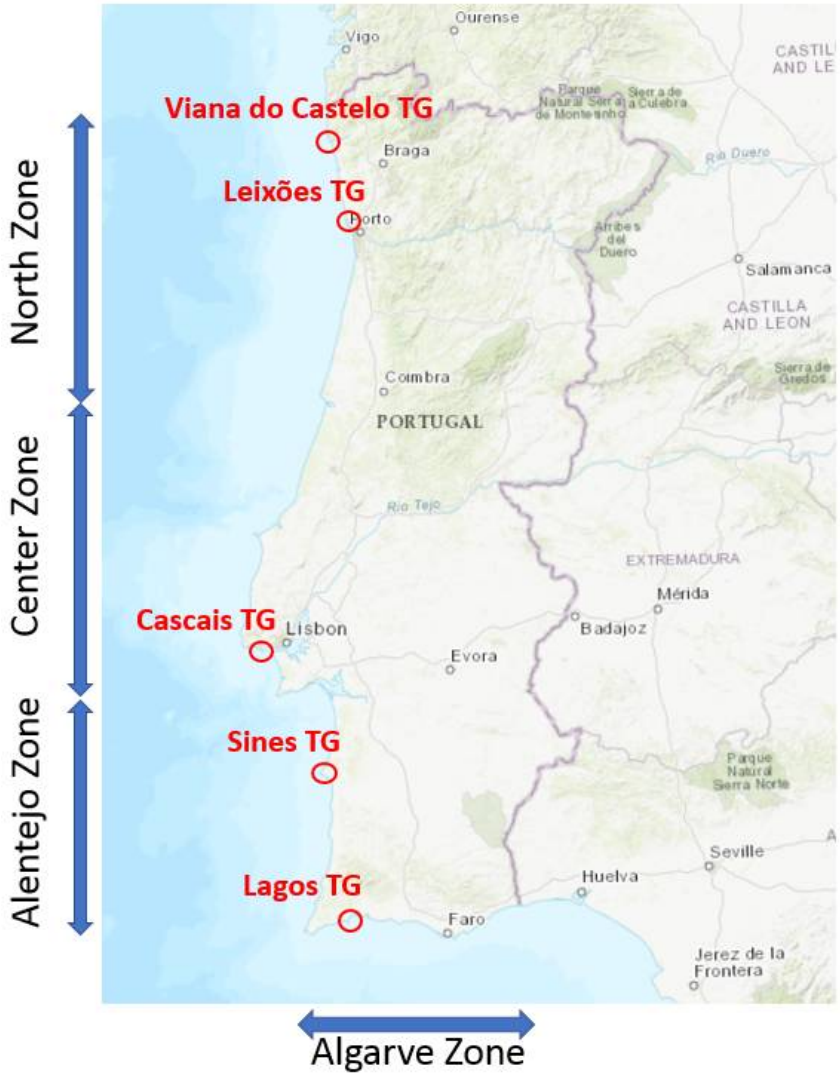

Figure 2. Location of the five TG used in the study: *Leixões*, *Cascais*, *Sines* and *Lagos* for the tide modeling and *Viana do Castelo* for storm surge analysis at the northern region.

2.1.3. Storm surge modelling

Storm Surge (SS) is the additional increase of the predicted astronomical tides caused by meteorological forcing due to storm events, through the joint effect of a lower atmospheric pressure, with a ratio of -1 cm/hPa, and the persistent effect of wind friction on the sea surface, depending on its direction and intensity. SS is a tide level disturbance, usually positive but can also be negative when high atmospheric pressure occurs, ranging from a few centimeters to several meters and that can last for hours to more than a day. In Portugal, according to an update study following the methodology of [18], which is based on the analysis of tide gauges data series from 1960 to 2018, the

Preprints (www.preprints.org) | NOT PEER-REVIEWED | Posted: 6 May 2019 doi:10.20944/preprints201905.0052.v1

Peer-reviewed version available at Geosciences 2019, 9, 239; doi:10.3390/geosciences9050239

maximum observed storm surge, along the west coast of Portugal mainland, exhibited average values ranging from 50 to 70 cm for the different TG, and maximums values of 80 cm to 1 m for long return periods (100 years or more). The maximum value detected by harmonic analysis was 82 cm in the *Viana do Castelo* TG (Figure 2) at October 15th, 1987, and 83 cm in the *Lagos* TG at March 4th, 2013. In the latter, such magnitude is only explained by the additional wave setup effect due to the TG localization and the SW wave direction of such storm event.

To evaluate and characterize the SS for the TG data series, a harmonic analysis was preformed, and the maximum storm surge series were updated for further analysis through the simple Gumbel distribution (Figure 3a to 3c).

The *Viana do Castelo* TG data set was used to assess the storm surge for the northern region (Figure 3a), due to the absence of enough data for the *Leixões* TG. The Cascais TG data set was applied for the central region storm surge assessment (Figure 3b), and the Lagos TG data set for Alentejo and Algarve regions (Figure 3c).

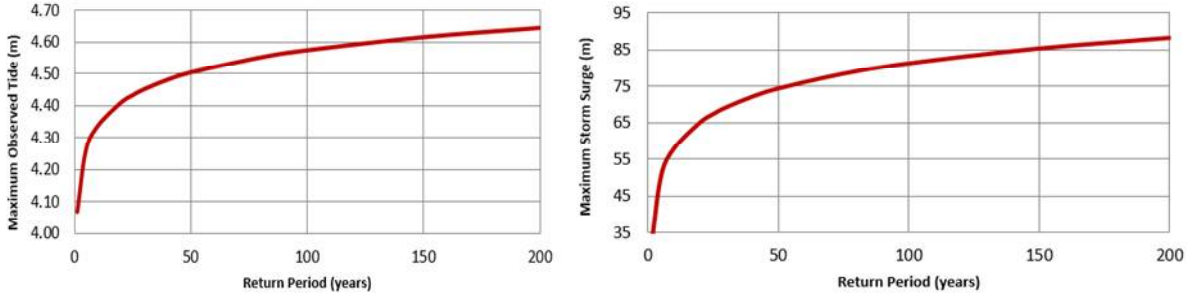

Figure 3a. Return period curves for the maximum observed tide (left), relative to the TG chart datum, and the maximum storm surge (right) for the *Viana do Castelo* TG (1978-2008 data series).

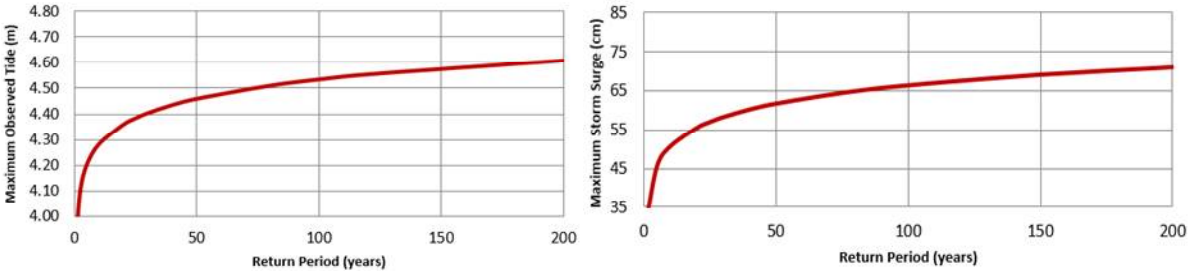

Figure 3b. Return period curves for the maximum observed tide (left), relative to the TG chart datum, and the maximum storm surge (right) for the *Cascais* TG (1959-2018 data series).

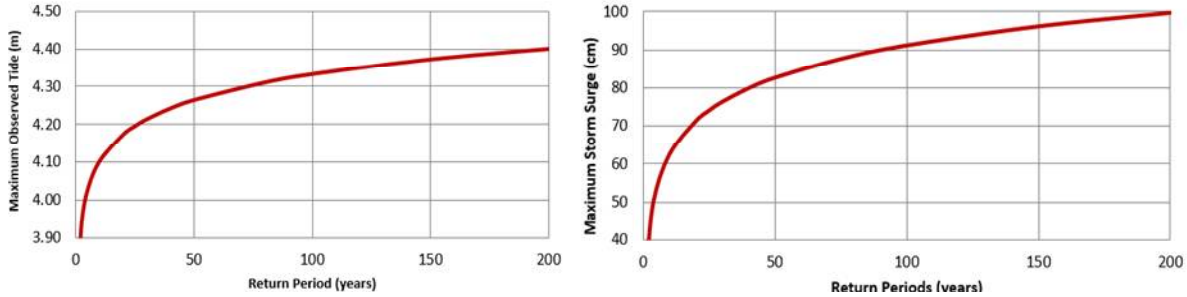

Figure 3c. Return period curves for the maximum observed tide (left), relative to the TG chart datum, and the maximum storm surge (right) for the *Lagos* TG (1986-2018 data series).

With this characterization, the maximum tide frequency, corresponding to the maximum tide and extreme storm surge joint probability, the 50, 100, and 200-year return periods (RP) were determined for the three TG at northern, central and southern regions (Table 1).

Preprints (www.preprints.org) | NOT PEER-REVIEWED | Posted: 6 May 2019 doi:10.20944/preprints201905.0052.v1

Peer-reviewed version available at Geosciences 2019, 9, 239; doi:10.3390/geosciences9050239

Table 1. Maximum tide height, relative to the respective TG chart datum, and storm surge (SS) for the 50, 100 and 200-year return periods, for previous three TG.

RP (year)	Viana do Castelo		Cascais		Lagos	
	MaxTide (m)	SS (cm)	MaxTide (m)	SS	MaxTide (m)	SS (cm)
50	4.50	75	4.46	62	4.26	82
100	4.57	81	4.53	66	4.33	91
200	4.65	88	4.61	71	4.40	100

2.1.4. Wave and wind setup

In addition to the tide forcing and the SS, the sea level (SL) extremes are also influenced by the settling effect resulting either from coastal waves in the nearshore breaking zone or from strong winds, particularly in inland waters where swell waves do not reach. Thus, to estimate sea surface extreme values near the coast, the wave setup must also be considered for open sea coastal areas and the wind setup for the inland water areas (estuaries and coastal lagoons).

The model that was used for the wave setup (S_0) follows the Direct Integration Method (DIM) applied by [19], which includes two setup components, a static component ($\bar{\eta}$) and a dynamic component $\hat{\eta}$:

$$S_0 = \bar{\eta} + \hat{\eta} \quad (1)$$

The static component is given by:

$$\bar{\eta} = 0.189 H_s \quad (2)$$

being H_s the significant wave height (highest third of the waves, $H_{1/3}$). The dynamic component is defined by the combination of the setup oscillation standard deviation (σ_1) and the incidence runup standard deviation (σ_2):

$$\hat{\eta} = 2.0\sqrt{\sigma_1^2 + \sigma_2^2} \quad (3)$$

where

$$\sigma_1 = 0.3 \frac{mH_s}{\sqrt{2\pi H_s / g L_s}} \quad (4)$$

and

$$\sigma_2 = 2.7 \left(\frac{H_s}{26.2}\right)^{0.8} \left(\frac{T_s}{20.0}\right)^{3.4} 3^{0.16} \left(\frac{m}{0.01}\right)^{0.2} \quad (5)$$

being m the average slope of the coast profile, the T_s the mean wave period.

The total effect of the wave setup coastal forcing corresponds to the overlapping of the incidence runup after the wave breaking. In this study, only average estimations of wave setup component, without the addition of the incidence runup effect, were considered due to the impossibility of determining an accurate beach profile along Portugal mainland coastline.

Based on the wave records time series of the *Leixões* and *Faro* wave buoys, a maximum analysis was preformed using the Gumbel function. From this analysis, H_s and T_s, corresponding to RP of 10 and 40 years (Table 2) of 6 and 7 m, were used for the calculation of the wave setup and added to the extreme tidal levels of 50 and 100 yr RP, respectively.

The wind setup S_v, applied only to inlets or inland waters, such as *Ria de Aveiro* and *Ria Formosa* (Algarve), and Tagus Estuary, results from the following expression [20]:

$$S_v = \rho_w \left(1.2^{-6} + 2.25^{-6}\left[1 - \frac{5.6}{V_{10}}\right]^2\right) V_{10}^2 \quad (6)$$

Preprints (www.preprints.org) | NOT PEER-REVIEWED | Posted: 6 May 2019 doi:10.20944/preprints201905.0052.v1

Peer-reviewed version available at Geosciences 2019, 9, 239; doi:10.3390/geosciences9050239

where V_{10} is the wind speed at 10 m above surface and ρ_w is the sea water density. Since no references were found for the region, an average wind speed of 38 km/h (10.6 m/s) was applied resulting into wind setup of S_v = 0.20 m.

Table 2. Significant heights (Hs) and mean wave periods (Ts), corresponding to the RP of 10 and 40 years, respectively.

Wave Height (H_s) (m)	Wave Period (T_s) (s)	Static Setup (m)	Dynamic Setup (m)	Total Setup (m)
6.0	14	1.13	0.79	1.9
7.0	15	1.32	0.92	2.2

2.2. Methodology for Coastal Flood Scenarios

2.1.1. Digital Terrain Model

The Digital Terrain Model (DTM) used in this study was obtained from the photogrammetric model provided by the DGT. The aerial photogrammetric survey for the basic cartographic data acquisition along Portugal Mainland coastal strip area, of approximately 513 400 ha, was carried out in 2008, with a spatial resolution of 2 m. In total, 4 139 files of elevation points (X, Y, Z), were processed for the DTM calculation.

In order to improve the computational performance of altimetric data processing, four different geographical zones were separately considered and the corresponding altimetric grid resampled at 20 m spatial resolution (Figure 2): North (from *Viana do Castelo* to *Figueira da Foz*), Center (from *Figueira da Foz* to *Cabo Espichel*), Alentejo (from *Sesimbra* to *Cabo de São Vicente*) and Algarve (from *Sagres* to *Vila Real Santo António*) (Table 1). This partition became also an advantage for the coastal forcing computation, once for each zone there are different estimate scenarios with the combination of Portuguese Atlantic coast SLR and the respective tide model, SS and wave setup estimations.

Table 3. Number of elevation points for each geographical zone.

Geographic Zone	Extension	# Elevation Points
North	*Viana do Castelo* to *Figueira da foz*	3 069 154
Center	*Figueira da Foz* to *Cabo Espichel*	5 845 401
Alentejo	*Sesimbra* to *Cabo de São Vicente*	1 149 289
Algarve	*Sagres* to *Vila Real Santo António*	1 744 278
Total		***11 808 122***

The positional quality control is indispensable in the production of flooding cartography due to the respective impact of an incorrect risk assessment. The DTM was produced by photogrammetry and, despite being a very efficient and accurate method, it is not free of errors. The respective data set was generated from raw data through filtering, by classification of points in "soil" and "non soil", and interpolation to fill the gaps. Errors may still occur during post-processing of the data. Therefore, quality control should detect errors and deviations, however it is very difficult to link certain errors (or its magnitude) to a concrete cause to be able to eliminate them [21].

For such purpose, the validation of the DTM was done based on a set of ground control points, in a total of 134 national geodetic marks, for which the altimetric values (orthometric base height - H_{GV}) are known and hence differences from the photogrammetric DTM heights (h_{DTM}) can be estimated:

$$error = h_{DTM} - H_{GV} \quad (7)$$

An overall mean square error of 56 cm was estimated with a sample of 134 control points for the entire coastal area. No shift, based on the obtained residual mean, was applied to the DTM, because the sample did not exhibit a normal random distribution due to the presence of large residuals.

Preprints (www.preprints.org) | NOT PEER-REVIEWED | Posted: 6 May 2019 doi:10.20944/preprints201905.0052.v1

Peer-reviewed version available at Geosciences 2019, 9, 239; doi:10.3390/geosciences9050239

Finally, the obtained DTM (Figure 4), for the whole coastal zone of Portugal Mainland, shows values between 0 m and 637.3 m with a spatial resolution of 20 m and with 56 cm of relative accuracy (precision).

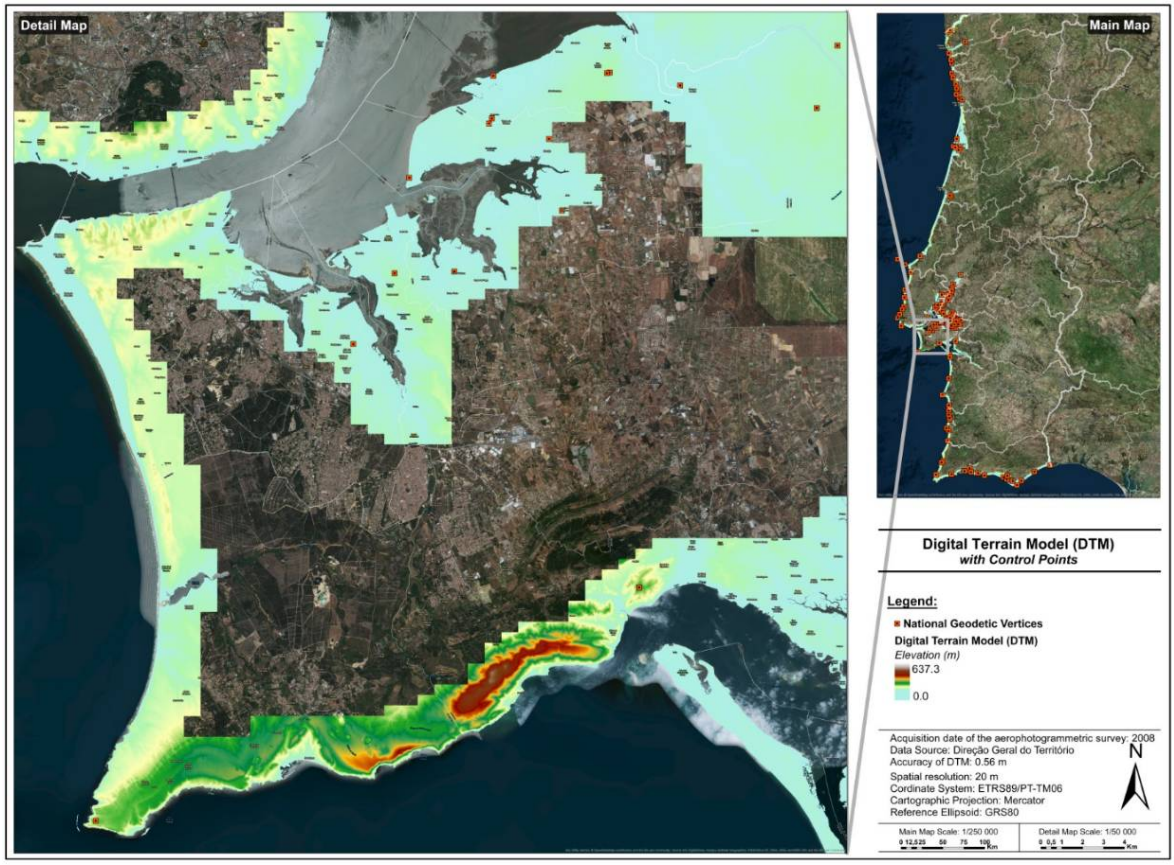

Figure 4. Digital Terrain Model of the Atlantic Coast of Portugal Mainland, with a spatial resolution of 20 m and 56 cm of relative accuracy estimated using the National Geodetic Network.

2.1.2. Methodology for the probabilistic cartography

Based on the methodology of [22], different SLR scenarios for 2050 and 2100, with different extreme events RP, and maximum tide levels were estimated based on tide historical data from the *Leixões*, *Cascais*, *Sines* and *Lagos* TG. Thus, each national wide scenario is a composition of four territorial zones: North, Center, Alentejo and Algarve. Except for the Cascais TG, that has the longest tide series, all the other TG (*Leixões*, *Sines* and *Lagos*) have shorter and incomplete data series for the 1970 - 2010 period.

Considering the ACPM SLR projection (Figure 1), the tide submersion percentiles were computed for the two epochs under study, 2050 and 2100. Adding the storm surge effect for two RP considered (50 and 100 years), as well as wave setup, to the predicted tide level submersion frequency for each reference TG, the flood levels are defined by Equations 8a and 8b.

$$Extreme\ Flood\ Level\_1 = Tide + StormSurge + SLR \quad (8a)$$

$$Extreme\ Flood\ Level_2 = Tide + StormSurge + SLR + SetUP \quad (8b)$$

From the resulting annual submersion percentile curves (Figure 5 shows only the case of Cascais TG), the elevations for the extreme flooding levels (EFL), corresponding to the 0.25% percentile (spring high-tides), were obtained.

Preprints (www.preprints.org) | NOT PEER-REVIEWED | Posted: 6 May 2019 doi:10.20944/preprints201905.0052.v1

Peer-reviewed version available at Geosciences 2019, 9, 239; doi:10.3390/geosciences9050239

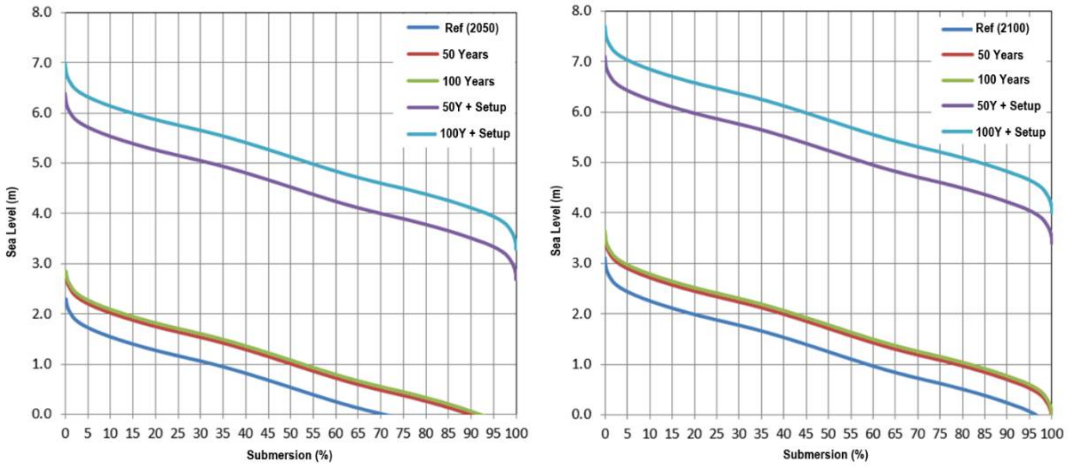

Figure 5. Cascais tide submersion percentile for the mean SL (blue) at epoch 2050 (left) and epoch 2100 (right), with storm surge (red and green) and wave setup (purple and light blue) for 50 and 100-year return periods.

To incorporate the SLR scenarios and their uncertainty into the vulnerability assessment, the Extreme Flood Hazard Index (EFHI) has been defined with five probability classes ranging from 1 (low hazard and low probability) to 5 (extreme hazard and high probability). The EFHI is then calculated by considering the uncertainty of the submersion frequency models, that result from the tides standard deviation estimation, storm surge, SLR and setup. Therefore, through Equations 8a and 8b, the uncertainty of extreme flood scenario is evaluated by:

$$\sigma_{Scenario\ EFL\ 1} = \sqrt{\sigma_{Tide}^2 + \sigma_{SS}^2 + \sigma_{SLR}^2} \quad (9a)$$

$$\sigma_{Scenario\ EFL\ 2} = \sqrt{\sigma_{Tide}^2 + \sigma_{SS}^2 + \sigma_{SLR}^2 + \sigma_{SetUp}^2} \quad (9b)$$

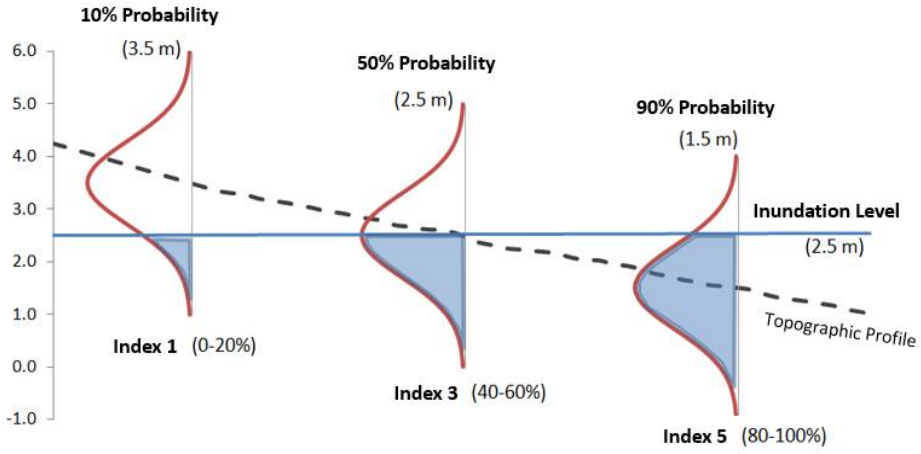

Figure 6. Method for the flooding probability calculation and the EFHI on a generic topographic profile (3.5 m, 2.5 m and 1.5 m), based on the highest tide level (h=2.5 m) and its uncertainty (adapted from [22]). Intermediate EFHI levels, 2 and 4, are located between index levels 1, 3 and 5.

The uncertainty value of each scenario depends on the projection year, therefore the scenario EFL_1 standard deviation obtained for the 2050 and 2100 epochs were 12 and 40 cm, respectively. Based on the uncertainties estimated by Equation 9a, the standard normal distribution curve is determined (Figure 6). This normal distribution curve has a conditional flood probability on the dimension of the topographic profile, which enables the determination of the probabilistic flood level for different topographic locations around the deterministic flood level (inundation level - central

Preprints (www.preprints.org) | NOT PEER-REVIEWED | Posted: 6 May 2019 doi:10.20944/preprints201905.0052.v1

Peer-reviewed version available at Geosciences 2019, 9, 239; doi:10.3390/geosciences9050239

projection of sea level). Subdividing the probability domain into five intervals of 20%, the EFHI is defined by a five-class range, from 1 (lowest probability, from 0.25 to 20%) to 5 (maximum probability, from 80 to 99.75%), related to coastal forcing (Table 4) and flooding hazard level.

Table 4. EFHI classification levels and respective conditional probability interval for a SLR scenario, relative to the respective central flooding elevation reference level.

Hazard Class Level	Very Low	Low	Moderate	High	Extreme
	1	2	3	4	5
Flood Probability	≤ 20%	20% - 40%	40% - 60%	60% - 80%	≥ 80%

3. Results

The costal flood hazard cartography is produced based in the GIS tools and supported by the most rigorous updated coastal DTM, referred in section §2.1.1. The flood hazard classification subdivided into five classes (from 1 – Very Low Hazard to 5 – Extreme Hazard), was then used to define the flooding scenarios cartography, from which the coastal physical vulnerability model is further developed and evaluated [11].

3.1. Probabilistic cartography of coastal flood

The flood scenarios assessment presented here is based on a probabilistic rather than a deterministic approach as explained in section §2.1.2 and is focused on the identification of areas with the flooding conditional probability for the future scenarios of SLR, for the time horizon of 2050 and 2100.

3.1.1. Year 2050

Table 5 shows the minimum and maximum values of each probabilistic interval corresponding to the five levels of flood hazard estimated for 2050. By intersecting these elevation interval levels with the DTM, the flooding areas for each scenario and geographical zone, are obtained and classified into five classes of flooding hazard, represented by a given scale color in a GIS map visualizer.

Table 5. Intervals for each EFHI level and respective probability for the 2050 SLR scenario for each geographic zone, relative to the central reference flooding elevation level (Ref).

Probability level		**2050, RP100, M+SS+SLR**			
		North & Center Ref=2.8 m		**Alentejo & Algarve Ref=2.7 m**	
		min	**max**	**min**	**max**
1 – Very Low	[0.25% to 20%]	2.90	3.25	2.80	3.15
2 – Low	[20% to 40%]	2.80	2.90	2.70	2.80
3 – Moderate	[40% to 60%]	2.75	2.80	2.65	2.70
4 – High	[60% to 80%]	2.65	2.75	2.55	2.65
5 – Extreme	[80% to 99.75%]	0.00	2.65	0.00	2.55
Scenario uncertainty		***12 cm***			

Table 6 presents the amount of area (km²) for each hazard class and each Portuguese coastal district for the 2050 epoch. It is possible to see that 903.2 km² of Portugal coastal zone are susceptible to be flooded in an extreme scenario with 100-year RP and being Lisbon the district with the largest flooding area (221.4 km²), followed by the Faro district (182.4 km²). Although Santarém isn't a coastal shoreline district, it is also affected by SLR scenarios due to the existence of an intertidal zone of Tagus Estuary.

Preprints (www.preprints.org) | NOT PEER-REVIEWED | Posted: 6 May 2019 doi:10.20944/preprints201905.0052.v1

Peer-reviewed version available at Geosciences 2019, 9, 239; doi:10.3390/geosciences9050239

Table 6. Flooding areas (in km²) for each EFHI class interval and respective probability, for the 2050 SLR scenario in each coastal district.

District	1 – Very Low [0.25% to 20%]	2 – Low [20% to 40%]	3 – Moderate [40% to 60%]	4 – High [60% to 80%]	5 – Extreme [80% to 99.75%]	Total [km²]
Aveiro	11.8	3.2	1.7	4.0	150.7	171.4
Beja	0.2	0.1	0.0	0.1	6.3	6.6
Braga	0.7	0.2	0.1	0.2	2.6	3.7
Coimbra	4.8	0.9	0.5	1.0	33.9	41.1
Faro	8.5	3.1	1.5	2.7	166.6	182.4
Leiria	3.5	0.9	0.5	1.1	14.2	20.2
Lisbon	12.3	4.1	2.4	5.8	196.8	221.4
Porto	0.4	0.1	0.0	0.1	1.9	2.5
Santarém	12.0	4.2	2.9	4.7	75.3	99.1
Setúbal	13.7	3.6	1.9	4.0	113.6	136.8
Viana do Castelo	2.8	1.1	0.4	0.9	12.7	17.9
Total	***70.7***	***21.5***	***12.0***	***24.5***	***774.4***	***903.2***

Figure 7 shows, for the ACPM, the 2050 coastal forcing scenarios probability, within a zoom of the Tagus Estuary.

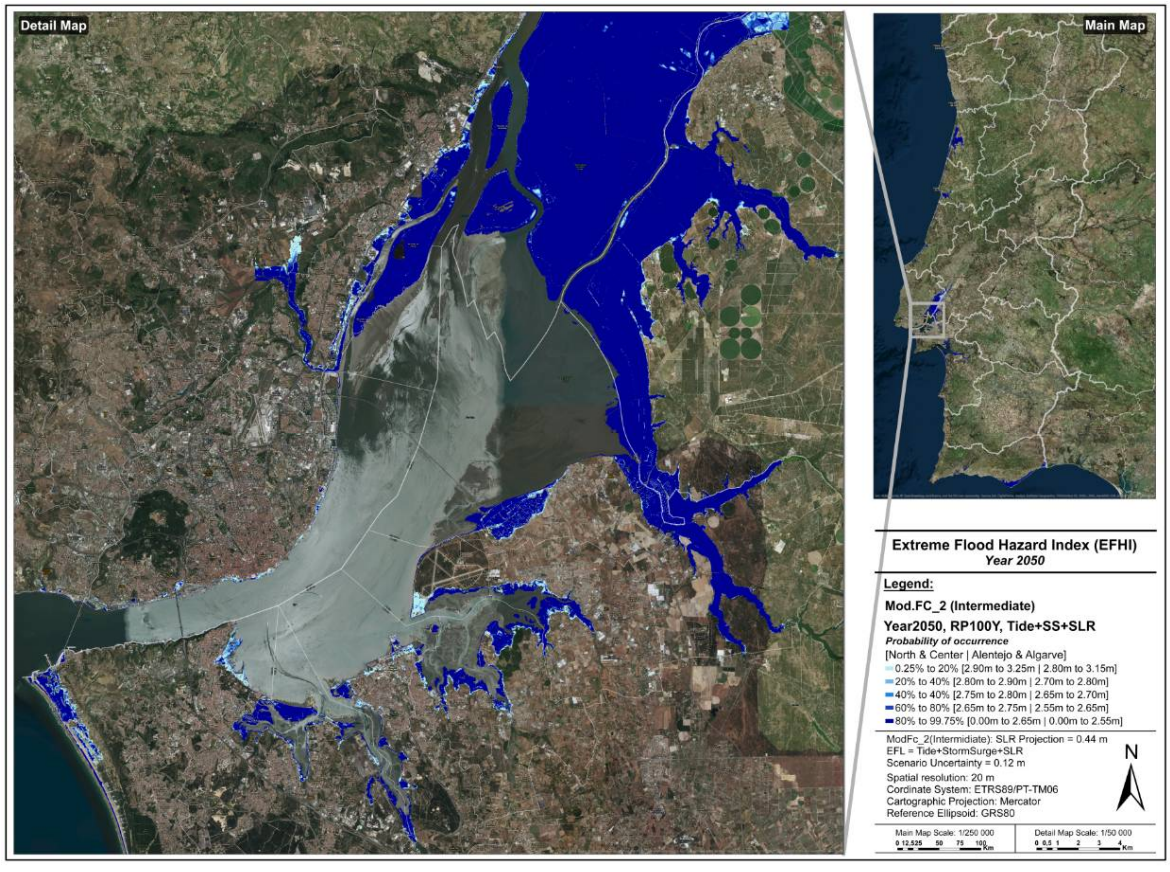

Figure 7. Portuguese coastal flooding extreme scenarios for 2050 SLR and 100-yr RP, within a zoom of the Tagus Estuary.

3.1.2. Year 2100

Table 7 shows, the minimum and maximum values of each probabilistic interval corresponding to the five levels of flood hazard estimated for 2100.

Preprints (www.preprints.org) | NOT PEER-REVIEWED | Posted: 6 May 2019 doi:10.20944/preprints201905.0052.v1

Peer-reviewed version available at Geosciences 2019, 9, 239; doi:10.3390/geosciences9050239

Table 7. Intervals for each EFHI level and respective probability for the SLR 2100 scenario for each geographic zone, relative to the central reference flooding elevation level (Ref).

Probability level		2100, RP100, M+SS+SLR			
		North & Center Ref=3.5 m		Alentejo & Algarve Ref=3.4 m	
		min	max	min	max
1 – Very Low	[0.25% to 20%]	3.95	4.85	3.85	4.75
2 – Low	[20% to 40%]	3.60	3.95	3.50	3.85
3 – Moderate	[40% to 60%]	3.35	3.60	3.25	3.50
4 – High	[60% to 80%]	3.00	3.35	2.90	3.25
5 – Extreme	[80% to 99.75%]	0.00	3.00	0.00	2.90
Scenario uncertainty		*40 cm*			

Table 8 presents the sum of areas for each hazard class and each Portuguese coastal district for the 2100 epoch. Besides, it is also shown that an area of 1146 km² has the probability of flood in 2100, and that 74.6% of that area is classified as extreme. The Lisbon district will be again the most affected with an area of 249.6 km² with probability of flood.

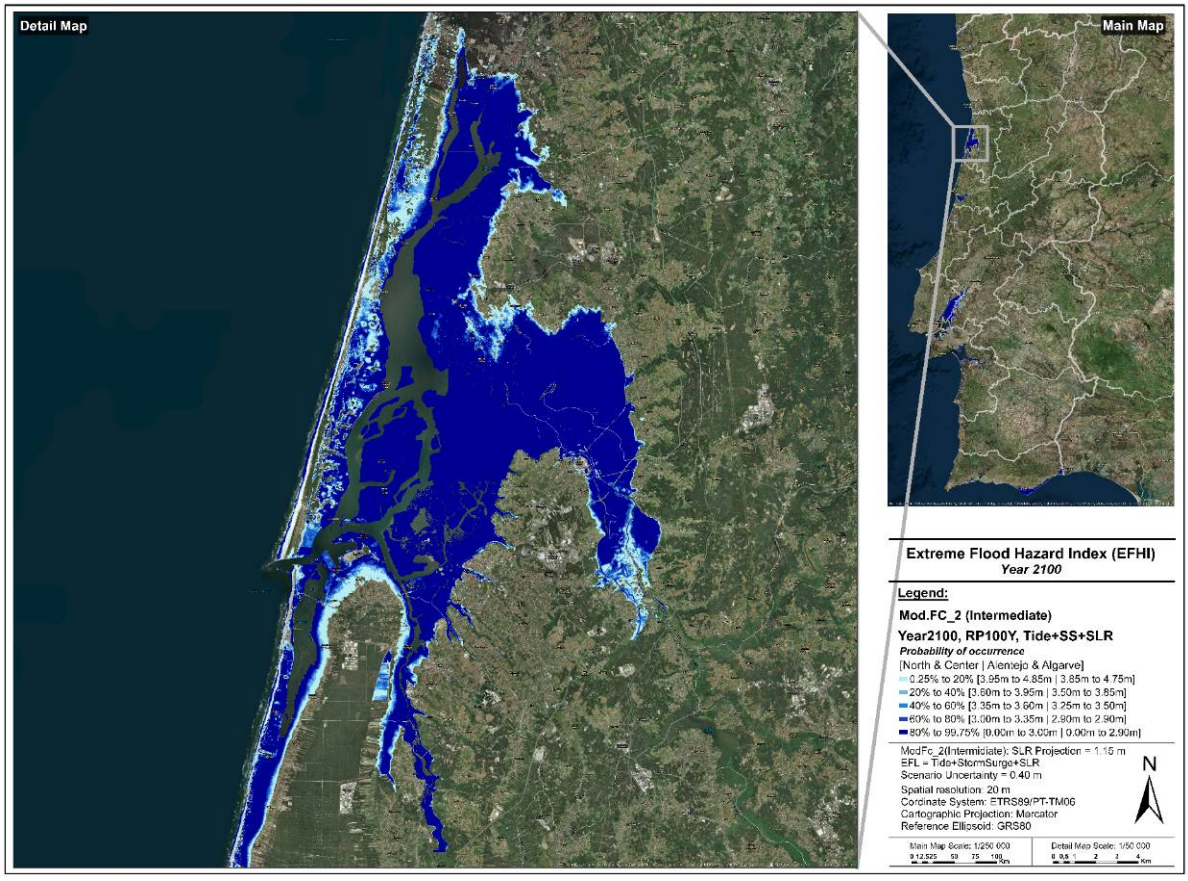

Figure 8. Portuguese coastal flooding extreme scenarios for 2100 SLR and 100-yr RP, within a zoom of the Aveiro inland lagoon (*Ria de Aveiro*).

Table 8. Flooding areas (in km²) for each EFHI class interval and respective probability, for the SLR 2100 scenario in each coastal district.

District	1 – Very Low [0.25% to 20%]	2 – Low [20% to 40%]	3 – Moderate [40% to 60%]	4 – High [60% to 80%]	5 – Extreme [80% to 99.75%]	Total [km²]

Aveiro	25.2	10.5	8.0	11.4	163.6	218.6
Beja	0.4	0.2	0.1	0.2	6.5	7.3
Braga	2.4	0.8	0.5	0.7	3.2	7.6
Coimbra	5.8	3.3	2.6	4.7	37.6	54.0
Faro	14.2	6.7	5.3	8.5	176.3	211.0
Leiria	7.1	3.3	2.4	3.5	17.8	34.1
Lisbon	10.5	8.2	6.6	11.2	213.2	249.6
Porto	2.0	0.6	0.4	0.4	2.2	5.7
Santarém	29.5	11.1	9.3	11.7	91.3	152.9
Setúbal	18.6	8.2	6.9	12.8	127.5	174.1
Viana do Castelo	7.1	3.1	2.1	2.9	15.9	31.1
Total	***122.8***	***56.1***	***44.1***	***68.0***	***855***	***1146***

Figure 8 shows, for ACPM, the 2100 coastal forcing scenarios probability, within a zoom of the *Ria de Aveiro*.

3.2. Probabilistic cartography of extreme coastal flood with wave and wind setup

The extreme flood scenario with setup (EFL_2 in Equation 8b), must be separated into open sea coastal areas (coastal shoreline), with the influence of ocean waves and consequently wave setup, and inland water areas, only influenced by wind setup, which requires a mask to apply both scenarios to the whole DTM in GIS.

Using the setup models values (wave setup presented in the Table 2), Table 9 shows the minimum and maximum values of each probabilistic interval corresponding to the five levels of flood hazard estimated for 2100. For inland water zones, a maximum wind setup of 20 cm was added to the values in Table 7. The scenario uncertainty was kept the same (40 cm), due to the difficulty in the estimation of the respective coupled scenario standard deviation. Knowing that the most accurate uncertainty would be higher than the one adopted, the larger the flooded area would be.

Figure 9 presents, for the Atlantic Coast of Portugal, the 2100 coastal forcing scenarios probabilistic map of Ria de Aveiro. Comparing Figure 8 with Figure 9, it is possible to observe some differences between them, specifically along the coastal shoreline and at the limits of the extreme arms of the lagoon. In the scenario with influence of wave and wind setup, there is a larger area with flooding probability, as it would be expected. This scenario is somehow realistic because storm surges can sometimes be accompanied by high energetic swell waves that generates a higher storm setup.

Preprints (www.preprints.org) | NOT PEER-REVIEWED | Posted: 6 May 2019 doi:10.20944/preprints201905.0052.v1

Peer-reviewed version available at Geosciences 2019, 9, 239; doi:10.3390/geosciences9050239

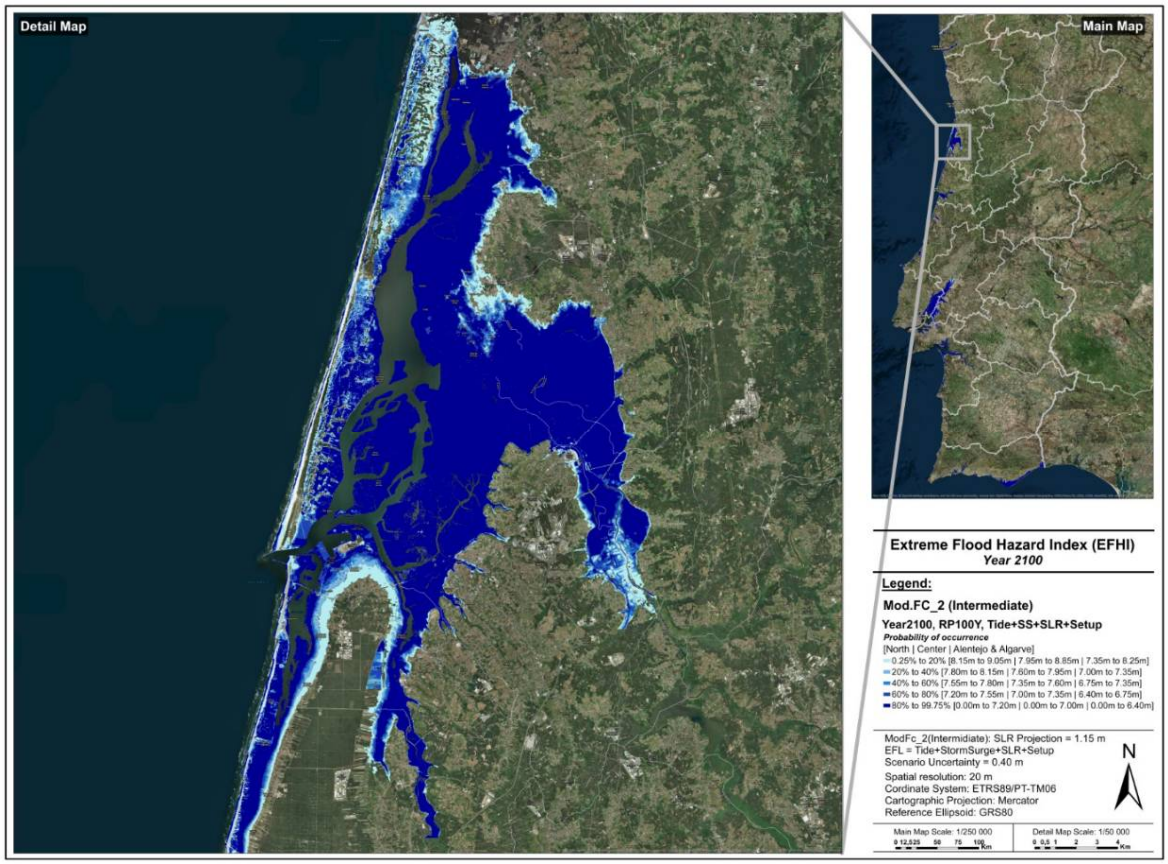

Figure 9. Portuguese coastal flooding extreme scenario with the influence of wave and wind setup, of for 2100 SLR and 100-yr RP, within a zoom of Aveiro inland lagoon (*Ria de Aveiro*).

Table 9. Intervals for each EFHI level and respective probability for the SLR 2100 scenario with the additional setup component for each geographic zone, relative to the central reference flooding elevation level (Ref).

		2100, RP100, M+SS+SLR+Setup					
Probability level		**North Ref=7.7 m**		**Center Ref=7.5 m**		**Alentejo & Algarve Ref=6.9 m**	
		min	max	min	max	min	max
1 – Very Low	[0.25% to 20%]	8.15	9.05	7.95	8.85	7.35	8.25
2 – Low	[20% to 40%]	7.80	8.15	7.60	7.95	7.00	7.35
3 – Moderate	[40% to 60%]	7.55	7.80	7.35	7.60	6.75	7.00
4 – High	[60% to 80%]	7.20	7.55	7.00	7.35	6.40	6.75
5 – Extreme	[80% to 99.75%]	0.00	7.20	0.00	7.00	0.00	6.40
Scenario uncertainty		*40 cm*					

5. Conclusions

The developed methodology allows the production of probabilistic coastal flooding cartography for any considered SLR projection, any coastal force model coupling and any DTM spatial resolution, based on a hydrostatic model basis and considering that the respective associated parameters uncertainties are provided or estimated.

Considering the Mod.FC_2b projection for the 2050 SLR with a SS of 50-yr RP for each TG zone, a total of 903 Km² of the ACPM is potentially affected by extreme flooding; being the districts of Lisbon, Faro and Aveiro the most affected, respectively, with 221, 182 and 172 km² of flooded area.

While for 2100, those values rise to 1146 Km² of total area and, respectively, 250, 211 and 219 Km² for the same most affected districts.

Knowing that the DTM represents the actual coastal morphology, without any erosion effect that is expected for future coastline retrieving, the present scenario for the coast shoreline with wave setup is underestimated. Due to the coastal retrieving, forced by the sedimentary deficit, the increase wave energy and its rotation caused by climate change, as well as, the increasing effect of SLR on wave forward breaking towards inland, the flood extension and respective impact in open coast shoreline areas will be certainly much greater than what is here estimated and presented.

As it is well known and widely studied, beach coastal areas are presently at high risk of erosion due to the sedimentary deficit and slightly increase wave energy coupled with SLR, but despite their economic and strategic importance, those are areas where the danger of SLR contributes less to the flooding vulnerability due to the low exposure of population and infrastructure, contrary to what is expected in the inland waters (river mouths, estuaries and ocean water lagoons) where the much higher exposure will contribute potentially to a considerable higher risk level.

The probabilistic flood mapping production allows not only to quantify and qualify the flooded area hazard for each scenario, but also, through the formulation and classification of the EFHI combined with other physical susceptibility parameters, the future evaluation of the coastal vulnerability mapping and the coastal risk assessment. These outputs are and will be fundamental for coastal planning adaptation within a sustainable gradual and collaborative strategy.

Results contribute greatly to the identification of areas that are most vulnerable to SLR and extreme events in the context of climate change, not just because it is the first SLR flood assessment for the whole Portugal Mainland, but also because the coastal flooding risk is assessed and the Directive 20007/60/CE objectives are implemented.

Funding: This research received no external funding.

Conflicts of Interest: The authors declare no conflict of interest.

References

1. Nerem, R.S.; Chambers, D.P.; Choe, C.; Mitchum, G.T. Estimating Mean Sea Level Change from the TOPEX and Jason Altimeter Missions. *Marine Geodesy* **2010**, *Volume 33*, pp.435–446. doi: 10.1080/01490419.2010.491031
2. Church, J.A.; White, N.J. Sea-Level Rise from the Late 19th to the Early 21st Century. *Surveys in Geophysics* **2011,** *Volume 32*, pp.585–602. doi: 10.1007/s10712-011-9119-1
3. Hay, C.C.; Morrow, E.; Kopp, R.E.; Mitrovica, J.X. Probabilistic reanalysis of twentieth-century sea-level rise. *Nature* **2015**, *Volume 517*, pp.481–484. doi: 10.1038/nature14093
4. Sweet, W.V.; Kopp, R.E.; Weaver, C.P.; Obeysekera, J.; Horton, R.M.; Thieler, E.R.; Zervas, C. Global and Regional Sea Level Rise Scenarios for the United States. *NOAA Technical Report*; Publisher: NOAA Silver Spring, Maryland, USA, **2017,** NOS CO-OPS 083.
5. Antunes, C. Assessment of sea level rise at west coast of Portugal Mainland and its projection for the 21st century. *J. Mar. Sci. Int.*, 7(3), 61. doi: 10.3390/jmse7030061.
6. Leuliette, E.W.; Scharroo, R. Integrating Jason-2 into a multiple-altimeter climate data record. *Marine Geology* **2010**, 33(sup 1), 504–517. doi: 10.1080/01490419.2010.487795.
7. Johnson, G.C.; Chambers, D.P. Ocean bottom pressure seasonal cycles and decadal trends from GRACE Release-05: Ocean circulation implications. *Journal of Geophysical Research* **2013**, 118(9), 228-240. doi: 10.1002/jgrc.20307.
8. Roemmich, D.; Gilson, J. The 2004–2008 mean and annual cycle of temperature, salinity, and steric height in the global ocean from the Argo Program. *Progress in Oceanography* **2009**, 82, 81–100. doi: 10.1016/j.pocean.2009.03.004.
9. McGrannahan, G.; Balk, D.; Anderson, B. The rising tide: assessing the risks of climate change and human settlements in low elevation coastal zones. *Environment & Urbanization* **2007**, 19(1), 17-37. doi: 10.1177/0956247807076960.
10. European Parliament; Council of the European Union. Floods Directive (2007/60/EC). *Official Journal of the European Union* **2007**, *Vol. 50 – L288*, pp. 27–34. ISSN: 1725-2555.

11. Rocha, C.S. Estudo e análise da vulnerabilidade costeira face a cenários de subida do nível do mar e eventos extremos devido ao efeito das alterações climáticas. Master Thesis, Faculdade de Ciências da Universidade de Lisboa, Portugal, **2016**.
12. Costa, M.S. Desenvolvimento de uma metodologia de avaliação de risco costeiro face aos cenários de alterações climáticas: aplicação ao Estuário do Tejo e à Ria de Aveiro. Master Thesis, Faculdade de Ciências da Universidade de Lisboa, Portugal, **2017**.
13. Orton, P.; Vinogradov, S.; Georgas, N.; Blumberg, A.; Lin, N.; Gornitz, V.; Little, C.; Jacob, K.; Horton, R. 581 New York City Panel on Climate Change 2015 report chapter 4: Dynamic coastal flood modeling. *Ann. N. 582 Y. Acad. Sci.* **2015**, 1336, 56-66.
14. Antunes, C.; Taborda, R. Sea Level at Cascais Tide Gauge: Data, Analysis and Results. Proceedings of the 10th International Coastal Symposium, Lisbon, Portugal, *Journal of Coastal Research* **2009**, *Special Issue 56*, pp. 218–222. doi: 10.2307/25737569.
15. Cabral, J. Neotectónica em Portugal Continental. *Inst. Geol. Min. Mem*. **1995**, 31, 265 p.
16. Antunes, C. Subida do Nível Médio do Mar em Cascais, revisão da taxa actual. Proceedings of 4as Jornadas de Engenharia Hidrográfica, Lisbon, Portugal, June 21-23; Instituto Hidrográfico, Eds.; **2016**, pp. 21–24. ISBN: 978-989-705-097-8
17. Antunes, C. Previsão de Marés dos Portos Principais de Portugal. FCUL Webpage, **2007**, Available online: http://webpages.fc.ul.pt/~cmantunes/hidrografia/hidro_mares.html.
18. Vieira, R.; Antunes, C.; Taborda, R. Caracterização da sobreelevação meteorológica em Cascais nos últimos 50 anos. Proceedings of 2as Jornadas de Engenharia Hidrográfica, Lisbon, Portugal, June 21-22; Instituto Hidrográfico, Eds.; **2012**, pp. 21–24. ISBN: 978-989-705-035-0
19. Federal Emergency Management Agency. Appendix D: Guidelines for Coastal Flooding Analysis and Mapping. In *Guidelines and Specifications for Flood Hazard Mapping Partners*, Federal Emergency Management Agency, Eds., Washington, D.C., **2002**, *Volume 3: Program Support*, p.384. www.fema.gov/fhm/dl_sgs.shtm.
20. Colvin, J.; Lazarus, S.; Splitt, M.; Weaver, R.; Taeb, P. Wind driven setup in east central Florida's Indian River Lagoon: Forcings and pameterizations. *Estuary, Coastal and Shelf Science* **2018**, 2013:40-48. doi: 10.1016/j.ecss.2018.08.004.
21. Höhle, J.; Höhle, M. Accuracy assessment of digital elevation models by means of robust statistical methods. *ISPRS Journal of Photogrammetry and Remote Sensing* **2009**, *Volume 64*, Issue 4, pp.398–406. doi: 10.1016/j.isprsjprs.2009.02.003
22. Marcy, D.; Brooks, W.; Draganov, K.; Hadley, B.; Haynes, C.; Herold, N.; McCombs, J.; Pendleton, M.; Schmid, K.; Sutherland, M.; Waters K. New Mapping Tool and Techniques for Visualizing Sea Level Rise and Coastal Flooding Impacts. Proceedings of the 2011 Solutions to Coastal Disasters Conference, Anchorage, Alaska, United States, June 26-29; American Society of Civil Engineers, Eds.; **2011**, pp. 474–490. doi: 10.1061/41185(417)42